IEEE Access
Multidisciplinary | Rapid Review | Open Access Journal

Received April 3, 2019, accepted April 18, 2019, date of publication April 26, 2019, date of current version May 7, 2019.

Digital Object Identifier 10.1109/ACCESS.2019.2912871

Particle Swarm Optimization-Based Gyro Drift Estimation Method for Inertial Navigation System

HONGYANG HE, BING ZHU, AND FENG ZHA
Department of Navigation Engineering, PLA Naval University of Engineering, Wuhan 430033, China
Corresponding author: Feng Zha (Zhafeng_1984@163.com)

This work was supported in part by the P.R.C. National Science Foundation of China under Grant 41804076 and Grant 41574069, in part by the Key R&D Program under Grant 2016YFB0501700 and Grant 2016YFB0501701, and in part by the Science Foundation of Hu Bei Province under Grant 2018CFB544.

ABSTRACT This paper proposes a novel gyro drift estimation method for the inertial navigation system (INS), which introduces the particle swarm optimization (PSO) algorithm into the error estimation problem. PSO-based estimation model is established. The position error and velocity error of INS are considered as the performance criterions of the PSO fitness function. Compared with the traditional gyro drift estimation methods, the advantages or contributions of the proposed method can be summarized as follows: 1) the proposed method does not require any prior information about inertial sensor error or observation noise; 2) particular motion for the carrier of INS is not needed, and; 3) the external information provided by other navigation systems could be discontinuous. The simulation experiments and field tests are performed, which validate the efficacy of the proposed method.

INDEX TERMS Inertial navigation system, particle swarm optimization, gyro drift estimation.

I. INTRODUCTION

An inertial navigation system utilizes the inertial properties of sensors mounted aboard the vehicle to execute the navigation function [1]–[6]. The system accomplishes this task through appropriate processing of the data obtained from force and inertial angular velocity measurements. Thus, an appropriate initialized inertial navigation system is capable of continuous determination of vehicle position and vehicle without the use of external radiation or optical information. Thus, inertial navigation systems have obvious advantages for military applications.

Short-term navigation accuracy of INS is relatively high. However the navigation error accumulates with time [7]–[9]. The main cause for the decrease of navigation accuracy is the gyro error of the inertial navigation system [10]–[12], which could usually be divided into constant error and random error. Depending on the calibration experiment in the calibration experiment, the constant error could be measured and compensated. The random error is caused by uncertain random disturbance, which could be further subdivided into random constant drift, random slope, random walk, etc [13]. Among them, the random constant drift, also known as gyro drift or gyro bias instability, affect the precision of inertial navigation system most.

The usual navigation errors of INS are longitude and latitude errors, east and north velocity errors, and the three attitude errors [14], [15]. Under the influence of gyro error, the longitude error diverges over time and the other six navigation errors oscillate regularly, the amplitudes of which will increase slowly. For the inertial navigation system that needs to work continuously for a long time, such as shipboard INS, the divergent errors are not acceptable. Therefore, estimation and compensation for the gyro error, especially gyro drift, are of great significance for the improvement of inertial navigation precision.

Traditionally, estimation for the gyro drift is mainly realized by Kalman Filter [16]–[20]. In [16], a modified adaptive Kalman gain correction algorithm is proposed to denoise IFOG signal. The Kalman gain is adaptively updated using the covariance matrix of innovation sequence. In [17], the Fiber Optic Gyroscope drift is modeled using an auto-regressive-moving-average time serials model. And the gyro drift is subsequently reduced using the proposed adaptive

The associate editor coordinating the review of this manuscript and approving it for publication was Lubin Chang.

unscented Kalman filter algorithm. Reference [18] proposes an improved double-factor adaptive Kalman filter called AMA-RWE-DFAKF to denoise fiber optic gyroscope (FOG) drift signal. In ideal conditions, Kalman Filter based estimation methods can effectively obtain the gyro drifts of inertial navigation system. However, these methods have limits: (1) Prior information of characteristics of inertial sensor errors are required; (2) Data of the integrated system should be continuous during the error estimation process; (3) In order to improve the observability of gyro drifts, some particular motion for the vehicle is required.

In view of the problems in traditional gyro drift estimation methods, a particle swarm optimization based gyro drift estimation method (PSOBE for short) for inertial navigation system is proposed in this paper. As we know, particle swarm optimization is a kind of intelligent algorithm, which is mainly used to search for the optimal solution to some complex optimization problem [21]–[23]. In this paper, the gyro drift of inertial navigation system is considered as the searched object for the particle swarm optimization. By this way, the gyro drift estimation problem is heuristically established as an optimal search problem. During the execution of the particle swarm optimization, a fitness function is needed to judge a particle or solution is good or not [24], [25]. For an inertial navigation system, in pure inertial state, larger gyro drifts lead to greater navigation errors. Meanwhile, all other things being equal, the smaller the navigation errors, the smaller the gyro drifts. From this point of view, navigation errors of INS can be used to establish the fitness function of the PSO algorithm when searching for the optimal gyro drifts. Per this line of thinking, the PSOBE method is proposed, the main idea of which can be presented as follows: Use PSO algorithm to search the gyro drifts of an INS. During the searching process, every particle contains a set of gyro drifts that needs to be evaluated. Compensate the raw gyro data of the INS with the gyro drifts in each particle to create corrected gyro data. The accuracy of pure inertial navigation by the corrected gyro data will be considered as the evaluation criteria for the performance of each particle.

Compared with the traditional Kalman filter based gyro drift estimation methods, the advantages of the proposed PSOBE method can be summarized as follows: (1) Prior information of inertial sensor errors is not needed; (2) Limitation for vehicle moving state is not required; (3) The data of the added navigation system, if needed, could be discontinuous.

The rest of this paper is organized as follows. Error characteristics of INS are analyzed in Section 2. In section 3, the fundamental principle of PSO is introduced and the PSOBE method is proposed. Simulation experiments and field tests are carried out in Section 4. Finally, conclusions are drawn in Section 5.

II. PROBLEM STATEMENT

Denote by n the local level navigation frame, an orthogonal reference frame aligned with east–north–up (ENU) geodetic axes; by b the SINS body frame, an orthogonal reference frame aligned within the IMU axes; by e the Earth frame, an Earth-centered Earth-fixed (ECEF) orthogonal reference frame; by i the chosen inertial frame.

The attitude, velocity and position rate equations in n-frame are, respectively, given by

$$\dot{\boldsymbol{C}}_{bn}^{n} = \boldsymbol{C}_{b}^{n}\boldsymbol{\Omega}_{nb}^{b} \tag{1}$$

$$\dot{\boldsymbol{V}}^{n} = \boldsymbol{C}_{b}^{n}\boldsymbol{f}^{b} - \left(2\boldsymbol{\omega}_{ie}^{n} + \boldsymbol{\omega}_{en}^{n}\right) \times \boldsymbol{V}^{n} + \boldsymbol{g}^{n} \tag{2}$$

$$\dot{L} = \frac{V_N}{R}, \quad \dot{\lambda} = \frac{V_E}{R\cos L} \tag{3}$$

where, $\boldsymbol{C}_{b}^{n}$ denotes the attitude matrix from the body frame to the navigation frame; $\boldsymbol{\omega}_{ib}^{b}$ the body angular rate measured by gyroscopes in the body frame; $\boldsymbol{\omega}_{in}^{n}$ the rotation rate of the navigation frame with respect to the inertial frame; $\boldsymbol{\omega}_{ie}^{n}$ the Earth rotation rate with respect to the inertial frame; $\boldsymbol{V}^{n} = [V_E, V_N, V_U]$ the velocity relative to the Earth; $[L, \lambda]$ the latitude and longitude; $\boldsymbol{f}^{b}$ the specific force measured by accelerometers in the body frame; R the radius of the Earth.

Error equations of INS can be deduced based on Equations (1)-(3), which are given by [5]

$$\dot{\boldsymbol{\phi}} = \boldsymbol{\phi} \times \boldsymbol{\omega}_{in}^{n} + \delta\boldsymbol{\omega}_{in}^{n} - \boldsymbol{C}_{b}^{n}([\boldsymbol{\delta K}_G] + [\boldsymbol{\delta G}])\boldsymbol{\omega}_{ib}^{b} - \boldsymbol{\varepsilon}^{n} \tag{4}$$

$$\begin{aligned}\delta\dot{\boldsymbol{V}}^{n} = {} & -\boldsymbol{\phi} \times \boldsymbol{\omega}_{in}^{n} + \boldsymbol{C}_{b}^{n}([\boldsymbol{\delta K}_G] + [\boldsymbol{\delta G}])\boldsymbol{f}^{b} + \boldsymbol{\delta V}^{n} \\ & \times \left(2\boldsymbol{\omega}_{ie}^{n} + \boldsymbol{\omega}_{en}^{n}\right) + \boldsymbol{V}^{n} \times \left(2\delta\omega_{ie}^{n} + \boldsymbol{\delta}\omega_{en}^{n}\right) + \nabla^{n}\end{aligned} \tag{5}$$

$$\delta\dot{L} = \frac{\delta V_N}{R} \tag{6}$$

$$\delta\dot{\lambda} = \frac{\delta V_E}{R}\sec L + \delta L\frac{V_E}{R}\tan L\sec L \tag{7}$$

where, $\varepsilon^{n} = [\varepsilon_E, \varepsilon_N, \varepsilon_U] = \boldsymbol{C}_{b}^{n}[\varepsilon_x, \varepsilon_y, \varepsilon_z]$ denotes the gyro drift in n-frame; $[\varepsilon_x, \varepsilon_y, \varepsilon_z]$ denotes the gyro drift in b-frame. $\nabla^{n} = [\nabla_E, \nabla_N, \nabla_U] = \boldsymbol{C}_{b}^{n}[\nabla_x, \nabla_y, \nabla_z]$ denotes the accelerometer drift in n-frame; $[\nabla_x, \nabla_y, \nabla_z]$ denotes the accelerometer drift in b-frame. $\phi = [\phi_x, \phi_y, \phi_z]$ denotes the misalignment attitude; $\delta\boldsymbol{V}^{n} = [\delta V_E, \delta V_N, \delta V_U]$ the velocity error; $[\delta L, \delta\lambda]$ the position errors.

$$\begin{bmatrix} \delta\dot{V}_E \\ \delta\dot{V}_N \\ \delta\dot{L} \\ \dot{\phi}_x \\ \dot{\phi}_y \\ \dot{\phi}_z \end{bmatrix} = \begin{bmatrix} 0 & 2\omega_{ie}\sin L & 0 & 0 & -g & 0 \\ -2\omega_{ie}\sin L & 0 & 0 & g & 0 & 0 \\ 0 & \frac{1}{R} & 0 & 0 & 0 & 0 \\ 0 & -\frac{1}{R} & 0 & 0 & \omega_{ie}\sin L & -\omega_{ie}\cos L \\ \frac{1}{R} & 0 & -\omega_{ie}\sin L & -\omega_{ie}\sin L & 0 & 0 \\ \frac{\tan L}{R} & 0 & \omega_{ie}\cos L & \omega_{ie}\cos L & 0 & 0 \end{bmatrix} \times \begin{bmatrix} \delta V_E \\ \delta V_N \\ \delta L \\ \phi_x \\ \phi_y \\ \phi_z \end{bmatrix} + \begin{bmatrix} \nabla_E \\ \nabla_N \\ 0 \\ \varepsilon_E \\ \varepsilon_N \\ \varepsilon_U \end{bmatrix} \tag{8}$$

According to Equations (4)-(7), the error characteristics of INS on a stationary base can be represented in matrix form as in (8), shown at the bottom of the previous page.

Thus, the time-domain expressions of the navigation errors can be given as:

$$\begin{aligned}&\delta V_E(t)\\&=\frac{g\sin L}{\omega_s^2-\omega_{ie}^2}(\sin\omega_{ie}t-\frac{\omega_{ie}}{\omega_s}\sin\omega_s t)\varepsilon_E\\&\quad+(\frac{\omega_s^2-\omega_{ie}^2\cos^2 L}{\omega_s^2-\omega_{ie}^2}\cos\omega_s t-\frac{\omega_s^2\sin^2 L}{\omega_s^2-\omega_{ie}^2}\cos\omega_{ie}t-\cos^2 L)\varepsilon_N\\&\quad+\frac{R}{2}\sin 2L(\frac{\omega_s^2}{\omega_s^2-\omega_{ie}^2}\cos\omega_{ie}t-\frac{\omega_{ie}^2}{\omega_s^2-\omega_{ie}^2}\cos\omega_s t-1)\varepsilon_U\\&\quad+\frac{\nabla_E}{\omega_s}\sin\omega_s t\end{aligned}\tag{9}$$

$$\begin{aligned}&\delta V_N(t)\\&=\frac{g}{\omega_s^2-\omega_{ie}^2}(\cos\omega_{ie}t-\cos\omega_s t)\varepsilon_E\\&\quad+\frac{g\sin L}{\omega_s^2-\omega_{ie}^2}(\sin\omega_{ie}t-\frac{\omega_{ie}^2}{\omega_s^2}\sin\omega_s t)\varepsilon_N\\&\quad+\frac{\omega_s\cos L}{\omega_s^2-\omega_{ie}^2}(\omega_{ie}\sin\omega_{ie}t-\omega_s)\varepsilon_U+\frac{\nabla_N}{\omega_s}\sin\omega_s t\end{aligned}\tag{10}$$

$$\begin{aligned}&\delta L(t)\\&=\frac{\omega_s^2}{\omega_s^2-\omega_{ie}^2}(\frac{1}{\omega_{ie}}\sin\omega_{ie}t-\frac{1}{\omega_s}\sin\omega_s t)\varepsilon_E\\&\quad+[\frac{\omega_{ie}\sin L}{\omega_s^2-\omega_{ie}^2}(\cos\omega_s t-\frac{\omega_s^2}{\omega_{ie}^2}\cos\omega_{ie}t)+\frac{\sin L}{\omega_{ie}}]\varepsilon_N\\&\quad+[\frac{\omega_s^2\cos L}{\omega_{ie}(\omega_s^2-\omega_{ie}^2)}\cos\omega_{ie}t-\frac{\omega_{ie}\cos L}{\omega_s^2-\omega_{ie}^2}\cos\omega_s t-\frac{\cos L}{\omega_{ie}}]\varepsilon_U\\&\quad+\frac{\nabla_N}{g}(1-\cos\omega_s t)\end{aligned}\tag{11}$$

$$\begin{aligned}&\delta\lambda(t)\\&=[\frac{\tan L}{\omega_{ie}}(1-\cos\omega_{ie}t)-\frac{\omega_{ie}\tan L}{\omega_s^2-\omega_{ie}^2}(\cos\omega_{ie}t-\cos\omega_s t)]\varepsilon_E\\&\quad+[\frac{(\omega_s^2-\omega_{ie}^2\cos^2 L)\sin\omega_s t}{\omega_s(\omega_s^2-\omega_{ie}^2)\cos L}-\frac{\omega_s^2\tan L\sin L\sin\omega_{ie}t}{\omega_{ie}(\omega_s^2-\omega_{ie}^2)\cos L}\\&\quad-t\cos L]\varepsilon_N\\&\quad+[\frac{\omega_s^2\sin L}{\omega_{ie}(\omega_s^2+\omega_{ie}^2)}\sin\omega_{ie}t-\frac{\omega_{ie}^2\sin L}{\omega_{ie}(\omega_s^2+\omega_{ie}^2)}\sin\omega_s t\\&\quad-t\sin L]\varepsilon_U\\&\quad+\frac{\nabla_E}{g\cos L}(1-\cos\omega_s t)\end{aligned}\tag{12}$$

$$\begin{aligned}&\phi_x(t)\\&=\frac{1}{\omega_s^2-\omega_{ie}^2}(\omega_s\cos\omega_s t-\omega_{ie}\sin\omega_{ie}t)\varepsilon_E\\&\quad+\frac{\omega_{ie}\sin L}{\omega_s^2-\omega_{ie}^2}(\cos\omega_{ie}t-\cos\omega_s t)\varepsilon_N\\&\quad+\frac{\omega_{ie}\cos L}{\omega_s^2-\omega_{ie}^2}(\cos\omega_s t-\cos\omega_{ie}t)\varepsilon_U-\frac{\nabla_N}{g}(1-\cos\omega_s t)\end{aligned}\tag{13}$$

$$\begin{aligned}&\phi_y(t)\\&=\frac{\omega_{ie}\sin L}{\omega_s^2-\omega_{ie}^2}(\cos\omega_s t-\cos\omega_{ie}t)\varepsilon_E\\&\quad+[\frac{\omega_s^2-\omega_{ie}^2\cos^2 L}{\omega_s(\omega_s^2-\omega_{ie}^2)}\sin\omega_s t-\frac{\omega_{ie}^2\sin^2 L}{\omega_s^2-\omega_{ie}^2}\sin\omega_{ie}t]\varepsilon_N\\&\quad+\frac{\omega_{ie}\sin 2L}{2(\omega_s^2-\omega_{ie}^2)}(\sin\omega_{ie}t-\frac{\omega_{ie}}{\omega_s}\sin\omega_s t)\varepsilon_U\\&\quad+\frac{\nabla_E}{g}(1-\cos\omega_s t)\end{aligned}\tag{14}$$

$$\begin{aligned}&\phi_z(t)\\&=[\frac{\omega_{ie}\sin L\tan L}{\omega_s^2-\omega_{ie}^2}(\cos\omega_s t-\cos\omega_{ie}t)+\frac{(1-\cos\omega_{ie}t)}{\omega_{ie}\cos L}]\varepsilon_E\\&\quad+\frac{\omega_{ie}^2\sin 2L-2\omega_s^2\tan L}{2(\omega_s^2-\omega_{ie}^2)}(\frac{1}{\omega_{ie}}\sin\omega_{ie}t-\frac{1}{\omega_s}\sin\omega_s t)\varepsilon_N\\&\quad+[\frac{\omega_s^2-\omega_{ie}^2\cos^2 L}{\omega_{ie}(\omega_s^2-\omega_{ie}^2)}\sin\omega_{ie}t-\frac{\omega_{ie}^2\sin^2 L}{\omega_s(\omega_s^2-\omega_{ie}^2)}\sin\omega_s t]\varepsilon_U\\&\quad+\frac{\nabla_E\tan L}{g}(1-\cos\omega_s t)\end{aligned}\tag{15}$$

According to Equations (9)-(15), the navigation errors caused by gyro drift fall into three classes: (1) oscillation error; (2) constant error; (3) accumulation error. The latter one is the key factor that undermines the system performance of INS. If the gyro drift could be accurately estimated and compensated, the navigation accuracy of INS is expected to be improved effectively.

III. PARTICLE SWARM OPTIMIZATION BASED GYRO DRIFT ESTIMATION METHOD

A. FUNDAMENTAL PRINCIPLE OF PARTICLE SWARM OPTIMIZATION

Particle swarm optimization (PSO) is a population based stochastic optimization technique developed by Dr. Eberhart and Dr. Kennedy in 1995, inspired by social behavior of bird flocking or fish schooling. In PSO, the potential solutions, called particles, fly through the problem space by following the current optimum particles. In this paper, a particle is a set of gyro drifts of INS.

The system is initialized with a population of random solutions and searches for optima by updating generations. The fitness function is established to evaluate the performance of each solution. Each particle keeps track of its coordinates in the problem space which are associated with the best solution, or fitness, it has achieved so far. This value is called personal best value, denoted by p_{best}. Another "best" value that is tracked by the particle swarm optimizer is the best value, obtained so far by any particle of all generations. This location is called global best value, denoted by g_{best}.

The particle swarm optimization concept consists of, at each time step, changing the velocity of each particle toward its p_{best} and g_{best} locations. Acceleration is weighted by a random term, with separate random numbers being generated for acceleration toward p_{best} and g_{best} locations.

The velocity and coordinate updating algorithm of the particle can be presented as follows:

$$v_{id}^{m+1} = \omega v_{id}^{m} + c_1 r_1 (p_{best}^{m} - x_{id}^{m}) + c_2 r_2 (g_{best}^{m} - x_{id}^{m}) \quad (16)$$

$$x_{id}^{m+1} = x_{id}^{m} + v_{id}^{m+1} \quad (17)$$

where, v and x are the velocity and coordinate of a particle. m is the generation number of the current population. $d = 1, 2, \ldots, N$ is the dimension of searching space. $i = 1, 2, \ldots, N$ is the population size. r_1 and r_2 are two random number between $[0, 1]$. c_1 and c_2 are learning factors which respectively represent the learning ability from the particle itself and other particles. Generally, c_1 and c_2 lie between $[0, 2]$. ω is the inertia weight coefficient, which is used to regulate the diversity of the particles. p_{best}^{m} and g_{best}^{m} are the personal best value and global best value of the current population. In order to improve the search efficiency, the value of v is usually limited between $[v_{\min}, v_{\max}]$. When the result of Equation (16) is out of the range, v should take the boundary value.

B. PROCEDURE OF THE PROPOSED ALGORITHM

As mentioned in section 2, accurate estimation for the gyro drift of INS is of great significance. Traditionally, the estimation is realized by Kalman filter based estimation methods, which have some inevitable constraints. In this paper, the estimation problem is creatively transferred to an optimal search problem, which is quite suited for PSO. Therefore, in this section, a particle swarm optimization based gyro drift estimation method is proposed. The structure of the proposed algorithm can be shown in Figure 1.

As shown in Figure 1, the procedure of the particle swarm optimization based gyro drift estimation method can be summarized as follows:

Step 1: The potential values of gyro drifts of INS are encoded in decimal numbers as the initial particles.

Step 2: Compensate the output of gyros with the gyro drifts in each particle to generate corrected gyro data. The corrected data is then used for navigation calculation based on inertial navigation differential equations.

Step 3: Based on the position error and velocity error of the INS with corrected gyro data, a fitness function is established to evaluate the performance of each particle. The detailed construction procedures of the fitness function will be illustrated latter in section C.

Step 4: Refresh the personal best value p_{best} and the global best value g_{best}.

Step 5: Refresh the velocity and coordinate of each particle in the problem space.

Step 6: If the terminating condition is not satisfied, the newly created population will be evaluated again and the process repeats.

Step 7: After 50 generations, the searching process ends. Execute inertial navigation calculation with the corrected gyro data by the optimum particle.

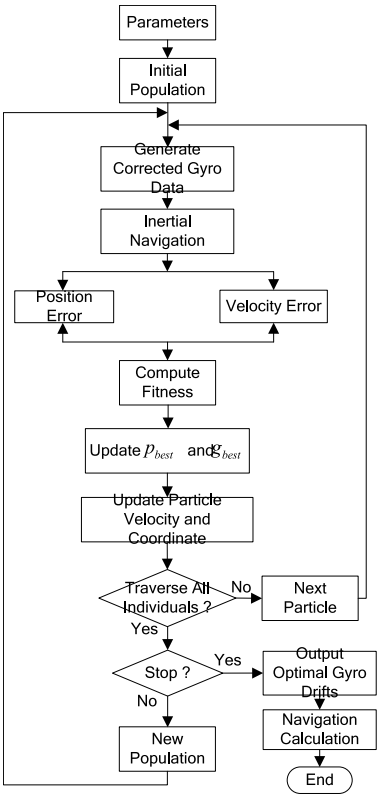

FIGURE 1. Structure of the proposed algorithm.

The expectation is that the fitness of the population will increase each round, and so by repeating this process for 50 rounds, very good solutions to this problem can be discovered.

C. ESTABLISH OF THE FITNESS FUNCTION

According to the analysis in section 2, gyro drift will affect the navigation precision of INS. As the position and velocity of the vehicle are relatively easy to be obtained by external information sources, the position error and velocity error of INS are considered as performance criterions in the particle swarm optimization fitness function to evaluate the performance of each particle during the gyro drift estimation process. According to the above analysis, the fitness function can be defined as follow:

$$J = \rho_1 \sum_{t_0}^{t_e} \left| e_{V_E}(t) \right| + \rho_2 \sum_{t_0}^{t_e} \left| e_{V_N}(t) \right| + \rho_3 \sum_{t_0}^{t_e} \left| e_{Lat}(t) \right| + \rho_4 \sum_{t_0}^{t_e} \left| e_{Lon}(t) \right| \quad (18)$$

where, t_0 denotes the start time of gyro drift estimation; t_e the end time of estimation; $e_{V_E}(t)$ the east velocity error; $e_{V_N}(t)$ the north velocity error; $e_{Lat}(t)$ the latitude error; $e_{Lon}(t)$ the longitude error; ρ_1, ρ_2, ρ_3, ρ_4 are weighted values.

IV. PERFORMANCE EVALUATION

A. SIMULATION EXPERIMENT

For the purposes of verifying the validity of the proposed PSOBE method, simulation experiments are carried out. Simulation conditions are given as:

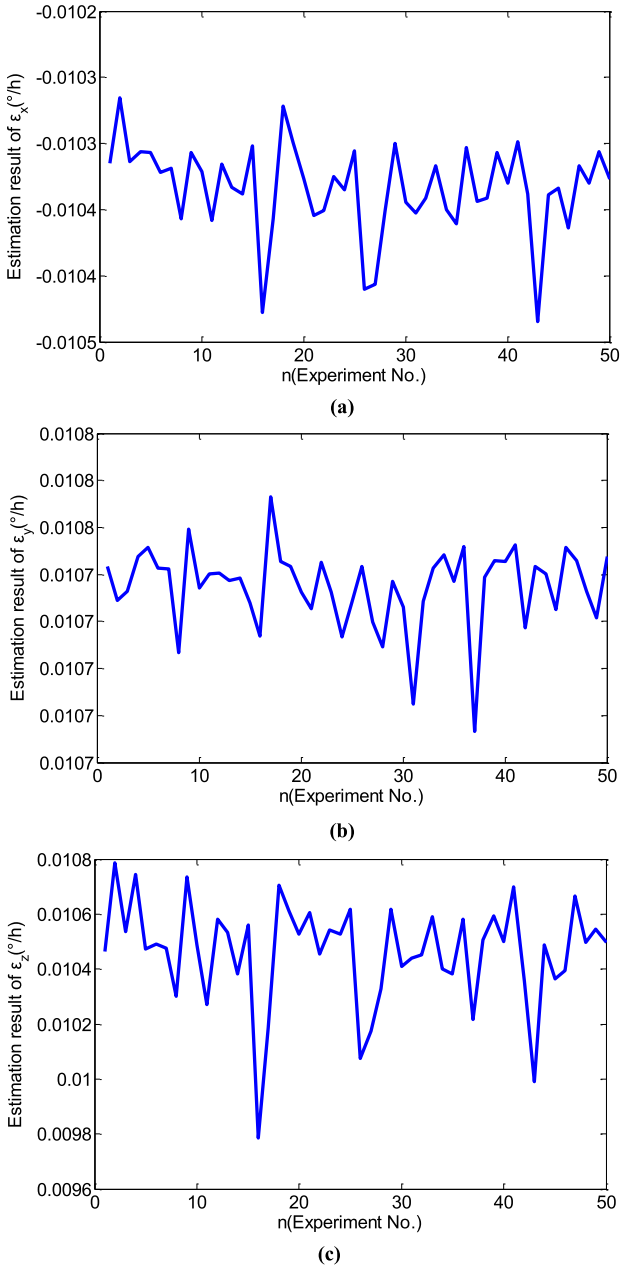

FIGURE 2. Gyro drifts searched out by the proposed PSOBE method for 50 simulation experiments. (a) Estimation results of ε_x. (b) Estimation results of ε_y. (c) Estimation results of ε_z.

Gyro drift: $\varepsilon_x = -0.01°/h$, $\varepsilon_y = 0.01°/h$, $\varepsilon_z = 0.01°/h$. The mean of gyro random walk is 0. And the standard deviation of gyro random walk is $0.001°/\sqrt{h}$. Accelerometer drift: $\nabla_x = 0.001m/s^2$, $\nabla_y = 0.001m/s^2$, $\nabla_z = 0.001m/s^2$.

The vehicle is assumed to be stationary and located on the surface of the earth at a latitude of 30.58°. Experiments are carried out in pure inertial state for 240 hours, in which the first 3 hours data is used for gyro drift estimation. The number of particles for one generation is 30. Parameters of PSO can be empirically assigned as follows: $c_1 = 1$, $c_2 = 1$, $r_1 = 1$, $r_2 = 1$, $\omega = 1$, $v_{\min} = -0.1/100$, $v_{\max} = 0.1/100$. The value ranges of gyro drifts are $\varepsilon_i \in [-0.03, 0.03](°/h)$, $i = x, y, z$. Parameters of fitness function in Equation (18) are: $\rho_1 = 1.0$, $\rho_2 = 1.0$, $\rho_3 = 1.0$, $\rho_4 = 10$. The searching process finishes after 50 generations.

TABLE 1. Statistics characteristics of gyro drifts.

gyro drift (°/h)	max	min	mean	std	reference
ε_x	-0.01032	-0.01048	-0.01038	$3.39*10^{-5}$	-0.01
ε_y	0.01077	0.01067	0.01073	$1.735*10^{-5}$	0.01
ε_z	0.01079	0.009786	0.01046	$1.913*10^{-4}$	0.01

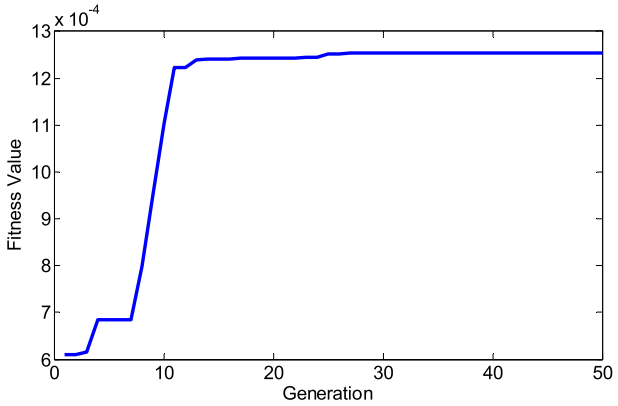

FIGURE 3. Optimization process of the fitness value f for the 1st test.

In order to verify the validity and repeatability of the estimation algorithm, 50 independent tests are carried out using the same simulation data. The results are shown in Figure 2 and their statistics are listed in Table 1. Taking the first test as an example, the varying processes of the fitness value f can be presented in Figure 3.

From Figure 2 and Table 1, it is clear that the difference among the error estimation results of the 50 independent tests is quite small, which shows that the proposed method has good repeatability and stability.

Define the estimation accuracy as:

$$Ac = (1 - \left|\frac{\eta_e - \eta_i}{\eta_i}\right|) \times 100\% \tag{19}$$

where η_e is the estimation value, η_i is the ideal value.

According to Table 1, the estimation accuracies of the three gyros for the 50 tests are all better than 90%. The average estimation accuracies of ε_x, ε_y and ε_z are respectively 96.2%, 92.7% and 95.4%. The results show that the proposed method has high estimation accuracy.

In order to illustrate the influence of the proposed PSOBE method to the precision of inertial navigation, navigation experiments are carried out, using the 240h simulation data. Two navigation schemes are compared:

Scheme 1: Traditional inertial navigation without compensation.

Scheme 2: Estimate the gyro drifts by the proposed PSOBE method. Compensate the output of gyros with the estimated gyro drifts. In this experiment, the gyro drifts used for compensation are the mean values in Table 1, that are

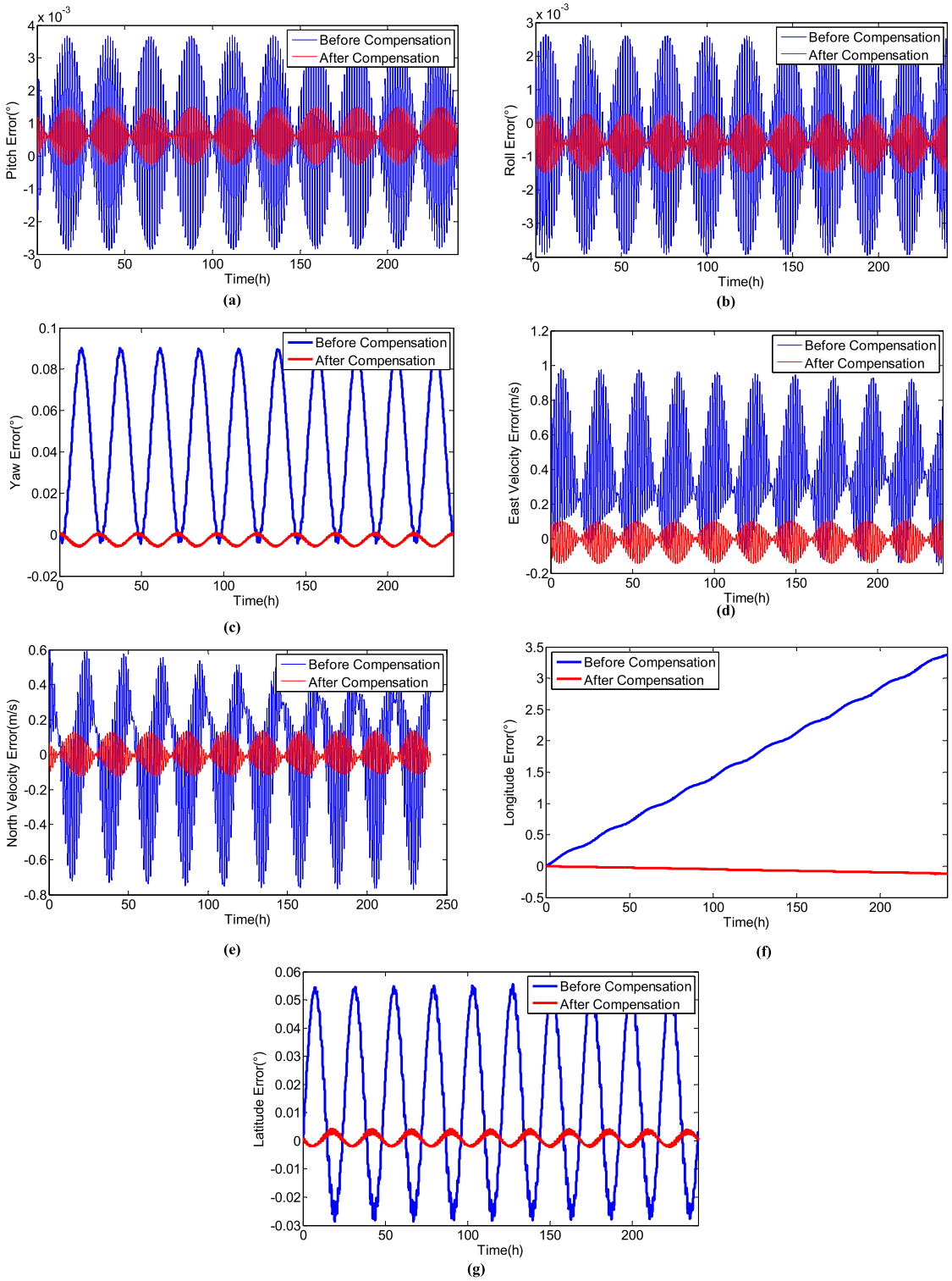

FIGURE 4. Navigation results by different schemes. (a) Pitch errors. (b) Roll errors. (c) Yaw errors. (d) East velocity errors. (e) North velocity errors. (f) Longitude errors. (g) Latitude errors.

$[\varepsilon_x, \varepsilon_y, \varepsilon_z] = [-0.01038, 0.01073, 0.01046](^\circ/h)$. The compensated data was then used for inertial navigation.

The experimental results are shown in Figure 4.

As shown in Figure 4, the blue lines denote the results of scheme 1, where the gyro drifts of INS were not estimated and compensated. The red lines denote the results of scheme 2, where the gyro drifts of INS were estimated by the proposed PSOBE method, which were then be compensated during the calculation of INS. The results show that the proposed method can effectively restrain the navigation errors of INS,

FIGURE 5. FOG SINS on the turntable.

TABLE 2. performance of the FOGs and accelerometers.

Item	gyroscope	accelerometer
Range	$\geq \pm 300^\circ/s$	$\pm 20g$
Bias	$\leq 0.02^\circ/h\ (1\sigma)$	$\leq 5\times10^{-4}\,g$
Bias Repeatability	$\leq 0.02^\circ/h\ (1\sigma)$	$\leq 2.5\times10^{-5}\,g\ (1\sigma)$
Scalar factor Repeatability	$10\,ppm\ (1\sigma)$	$\leq 3.5\times10^{-5}\ (1\sigma)$
Random walk	$\leq 0.005^\circ/\sqrt{h}$	——

which also demonstrates from another point of view that the proposed PSOBE method can accurately estimate the gyro drifts of INS.

B. FIELD TEST

In this section, the performance of the proposed PSOBE method is evaluated using field test data. The used field test data was collected from navigation-grade strapdown inertial navigation system (SINS) which is equipped with a triad of fiber optic gyroscopes and accelerometers. The fiber optic gyroscope (FOG) SINS is installed on the double-axis turntable as shown in Figure 5 with a latitude of 30.58° and a longitude of 114.2429°. The specifications of the inertial sensors of are listed in Table 2. The SINS provides raw IMU measurements at 100 Hz.

Parameters of PSO can be empirically assigned as follows: $c_1 = 1$, $c_2 = 1$, $r_1 = 1$, $r_2 = 1$, $\omega = 1$, $v_{\min} = -0.1/100$, $v_{\max} = 0.1/100$. Parameters of fitness function in Equation (18) are: $\rho_1 = 1.0$, $\rho_2 = 1.0$, $\rho_3 = 1.0$, $\rho_4 = 10$. The value ranges of gyro drifts are $\varepsilon_i \in [-0.03, 0.03](^\circ/h)$, $i = x, y, z$. The population size is 30. The evolutional generation is 50. The first 3 hours data is used for gyro drift estimation.

In order to verify the validity and repeatability of the estimation algorithm, 50 independent tests are carried out using the same field test data. The results are shown in Figure 6 and their statistics are listed in Table 3.

As shown in Figure 6 and Table 3, the consistency of the estimation results by the field test data is very good. Therefore, it can be concluded that the proposed PSOBE method is with good repeatability and stability. The estimation accuracy could be verified by the following navigation

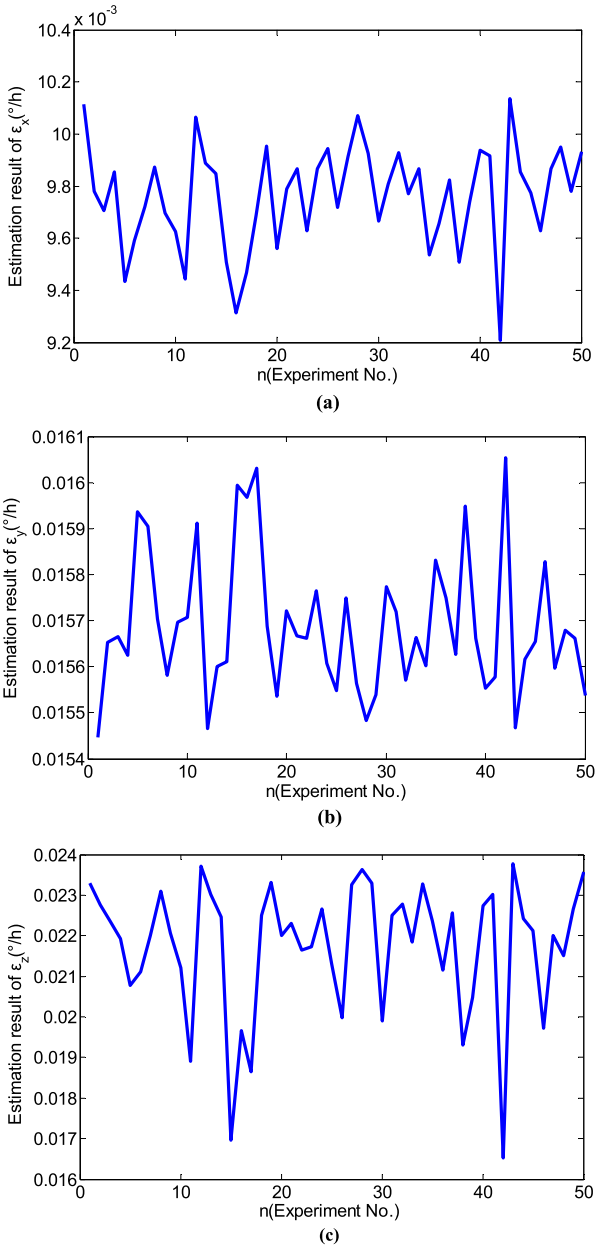

FIGURE 6. Gyro drifts searched out by the proposed PSOBE method for 50 field tests. (a) Estimation results of ε_x. (b) Estimation results of ε_y. (c) Estimation results of ε_z.

TABLE 3. Statistics characteristics of gyro drifts.

gyro drift (°/h)	mean	max	min	std
ε_x	0.009763	0.01014	0.009207	$2.005*10^{-4}$
ε_y	0.01569	0.01605	0.01545	$1.516*10^{-4}$
ε_z	0.02176	0.02377	0.01652	$1.65*10^{-3}$

experiments. And the results are shown in Figure 7, in which two navigation schemes are compared:

Scheme 1: Traditional inertial navigation without compensation.

Scheme 2: Estimate the gyro drifts by proposed PSOBE method. Compensate the output of gyros with the estimated

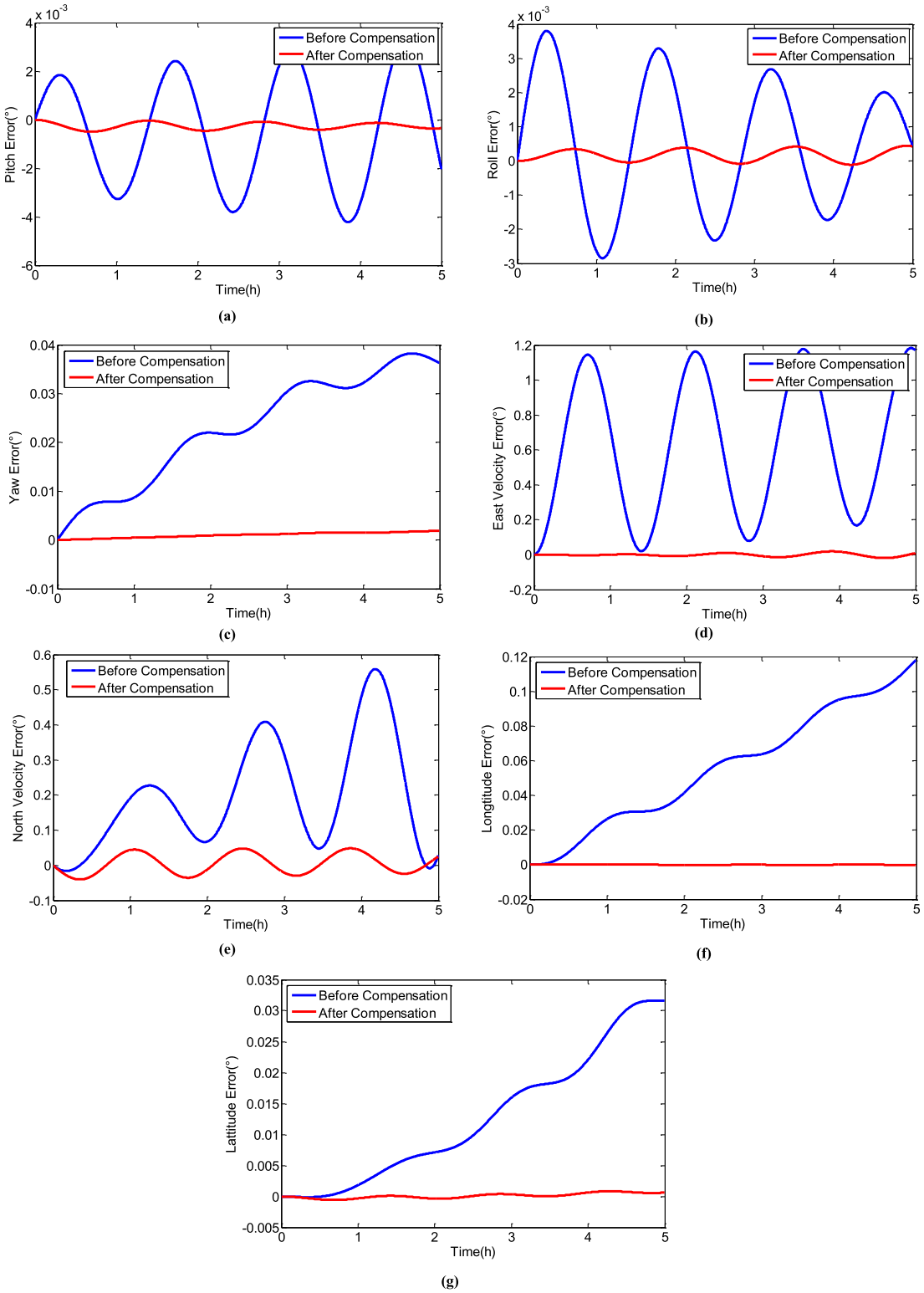

FIGURE 7. Navigation results by different schemes. (a) Pitch errors. (b) Roll errors. (c) Yaw errors. (d) East velocity errors. (e) North velocity errors. (f) Longitude errors. (g) Latitude errors.

gyro drifts. In this experiment, the gyro drifts used for compensation are the mean values in Table 3, that are $[\varepsilon_x, \varepsilon_y, \varepsilon_z] = [0.009763, 0.01569, 0.02176](^\circ/h)$. The compensated data was then used for inertial navigation.

In Figure 7, blue lines denote the navigation errors by Scheme 1, where the gyro drifts were not compensated; red lines denote the navigation errors by Scheme 2. It is clear that, by compensating the output of gyros with the estimated

gyro drifts, the navigation accuracy of the inertial navigation system in pure inertial state is significantly improved. The oscillation errors and accumulation errors of the inertial navigation system are dramatically decreased. As the navigation error of INS is closely related to the gyro errors, of which the greatest impact on long-term navigation precision is the gyro drift, it can be concluded that the proposed PSOBE method can effectively estimate the gyro drift of inertial navigation system. On this basis, the pure inertial navigation accuracy could be dramatically improved.

V. CONCLUSION

Estimation for gyro drift with high accuracy is of great significance for the improvement of navigation precision of INS in pure inertial state. Traditional error estimation methods require continuous external information, prior information of errors and some particular motion. When any of the above conditions are not met, the performance of the traditional error estimation methods cannot be guaranteed. In view of the problems in traditional methods, a particle swarm optimization based gyro drift estimation method for inertial navigation system is proposed in this paper. The particle swarm optimization method is introduced to solve the gyro drift estimation problem. The position error and velocity error of INS are considered as performance criterions in the particle swarm optimization fitness function. The error estimation problem is then transferred to an optimal search problem. Consequently, some problems existing in traditional methods could be resolved. In order to verify the validity of the proposed method, simulation experiments and field tests were carried out. Experiment results show that the proposed method can effectively estimate the gyro drift of the inertial navigation system without any prior information about the inertial sensor error and observation noise. Particular motion for the vehicle is not needed. And as the navigation error parameters in Equation (18) do not have to be continuous, the proposed method can also achieve a high precision estimation, even when the external added information is intermittently unavailable. In conclusion, the proposed PSOBE method can make up for the deficiencies in traditional error estimation methods and can be used simultaneously with the traditional methods to improve the reliability and stability of the gyro drift estimation. As a consequence, the navigation precision of INS can be improved accordingly.

REFERENCES

[1] D. H. Titterton and J. L. Weston, *Strapdown Inertial Navigation Technology*, 2nd ed. London, U.K.: IET, 2004.
[2] S. Guo, J. Xu, and H. He, "External velocity aided coarse attitude and position alignment for dynamic SINS," *IEEE Access*, vol. 6, pp. 15099–15105, 2018.
[3] F. Li, J. Xu, and H. He, "Backtracking velocity denoising based autonomous in-motion initial alignment," *IEEE Access*, vol. 6, pp. 67144–67155, 2018.
[4] J. Li, J. Xu, L. Chang, and F. Zha, "An improved optimal method for initial alignment," *J. Navigat.*, no. 67, no. 4, pp. 727–736, 2014.
[5] Y. Qin, *Inertial Navigation*. Beijing, China: Science Press, 2010.
[6] K. Li, P. Gao, X. Wang, and L. Wang, "Analysis and experiment of error restraint principle in an inertial navigation system with inertial sensors rotation," *Int. J. Sensor Netw.*, vol. 21, no. 2, pp. 127–136, 2016.
[7] H. Hongyang, X. Jiangning, Q. Fangjun, and Z. Feng, "Research on generalized inertial navigation system damping technology based on dual-model mean," *Proc. Inst. Mech. Eng. G, J. Aerosp. Eng.*, vol. 230, no. 8, pp. 1518–1527, Aug. 2015.
[8] W. Sun, D. Wang, L. Xu, and L. Xu, "MEMS-based rotary strapdown inertial navigation system," *Measurement*, vol. 46, no. 8, pp. 2585–2596, Oct. 2013.
[9] B. Wang, Q. Ren, Z. Deng, and M. Fu, "A self-calibration method for nonorthogonal angles between gimbals of rotational inertial navigation system," *IEEE Trans. Ind. Electron.*, vol. 62, no. 4, pp. 2353–2362, Apr. 2015.
[10] P. D. Groves, *Principles of GNSS, Inertial, and Multisensor Integrated Navigation Systems*. Norwood, MA, USA: Artech House, 2008.
[11] L. Wang, K. Li, L. Wang, and J. Gao, "Identifying Z-axis gyro drift and scale factor error using azimuth measurement in fiber optic gyroscope single-axis rotation inertial navigation system," *Proc. SPIE*, vol. 56, no. 2, 2017, Art. no. 024102.
[12] Z. Zheng, S. Han, J. Yue, and L. Yuan, "Compensation for stochastic error of gyros in a dual-axis rotational inertial navigation system," *J. Navigat.*, vol. 69, no. 1, pp. 169–182, 2016.
[13] G. Xiaolin and F. Jiancheng, "Improved method for measuring gyro constant drift on line in SINS," *Chin. J. Sci. Instrum.*, vol. 32, no. 4, pp. 756–762, 2011.
[14] Q. Fangjun, H. Hongyang, and X. Jiangning, "Phase modulation-based SINS damping method for autonomous vehicles," *IEEE Sensors J.*, vol. 18, no. 6, pp. 2483–2493, Mar. 2018.
[15] Y. Jia, S. Li, Y. Qin, and R. Cheng, "Error analysis and compensation of MEMS rotation modulation inertial navigation system," *IEEE Sensors J.*, vol. 18, no. 5, pp. 2023–2030, Mar. 2018.
[16] M. Narasimhappaa, S. L. Sabat, R. Peesapati, and J. Nayak, "An innovation based random weighting estimation mechanism for denoising fiber optic gyro drift signal," *Optik-Int. J. Light Electron Opt.*, vol. 125, no. 3, pp. 1192–1198, 2014.
[17] M. Narasimhappa, J. Nayak, M. H. Terra, and S. L. Sabat, "ARMA model based adaptive unscented fading Kalman filter for reducing drift of fiber optic gyroscope," *Sens. Actuators A, Phys.*, vol. 251, pp. 42–51, Nov. 2016.
[18] G. Yang, Y. Liu, M. Li, and S. Song, "AMA- and RWE-based adaptive Kalman filter for denoising fiber optic gyroscope drift signal," *Sensors*, vol. 15, no. 10, pp. 26940–26960, 2015.
[19] S. Y. Cho, "IM-filter for INS/GPS-integrated navigation system containing low-cost gyros," *IEEE Trans. Aerosp. Electron. Syst.*, vol. 50, no. 4, pp. 2619–2629, Oct. 2014.
[20] Y. Zhong, S. Gao, and W. Li, "A quaternion-based method for SINS/SAR integrated navigation system," *IEEE Trans. Aerosp. Electron. Syst.*, vol. 48, no. 1, pp. 514–524, Jan. 2012.
[21] R. V. Kulkarni and G. K. Venayagamoorthy, "Particle swarm optimization in wireless-sensor networks: A brief survey," *IEEE Trans. Syst., Man, Cybern. C, Appl. Rev.*, vol. 41, no. 2, pp. 262–267, Mar. 2011.
[22] V. Roberge, M. Tarbouchi, and G. Labonte, "Comparison of parallel genetic algorithm and particle swarm optimization for real-time UAV path planning," *IEEE Trans. Ind. Informat.*, vol. 9, no. 1, pp. 132–141, Feb. 2013.
[23] J. E. Onwunalu and L. J. Durlofsky, "Application of a particle swarm optimization algorithm for determining optimum well location and type," *Comput. Geosci.*, vol. 14, no. 1, pp. 183–198, Jan. 2010.
[24] M. Collotta, G. Pau, and V. Maniscalco, "A fuzzy logic approach by using particle swarm optimization for effective energy management in IWSNs," *IEEE Trans. Ind. Electron.*, vol. 64, no. 12, pp. 9496–9506, Dec. 2017.
[25] H. Han, X. Wu, L. Zhang, Y. Tian, and J. Qiao, "Self-organizing RBF neural network using an adaptive gradient multiobjective particle swarm optimization," *IEEE Trans. Cybern.*, vol. 49, no. 1, pp. 69–82, Jan. 2019. doi: 10.1109/TCYB.2017.2764744.

Authors' photographs and biographies not available at the time of publication.